

# **Comparative study of impact and static indentation tests on particulate filled thermoplastic fluoropolymer coatings**

Y. Xu<sup>\*+</sup> and B. G. Mellor

Materials Research Group  
Engineering Sciences  
University of Southampton  
Highfield, Southampton  
SO17 1BJ, UK

## **Abstract**

This study investigates the performance of particulate filled thermoplastic fluoropolymer coatings under both dynamic impact tests and static indentation tests. An instrumented impact testing rig was used to measure the impact energy, impact velocity, acceleration and

---

\* Corresponding author: Tel.: +44 1895 265883; fax: +44 1895 269861.  
Email address: [yanmeng.xu@brunel.ac.uk](mailto:yanmeng.xu@brunel.ac.uk) (Y. Xu)

<sup>+</sup> Current address: School of Engineering and Design, Brunel University, Uxbridge UB8 3PH, UK.

impact force during the impact tests. Coating samples with different thicknesses of coating layers and steel substrate were impact tested to investigate the effect of coating and substrate thickness on the impact response and damage to the coatings. The data obtained from the dynamic tests were used to calculate the Meyer hardness values of the coating and compared with the Meyer hardness results obtained from Brinell indentation tests on the coating. The Meyer index  $m$  was similar under dynamic impact and static indentation testing conditions. The Meyer hardness calculated from the impact tests does not change markedly as a function of depth of penetration normalised to the thickness of coating whereas the Brinell hardness increases with the depth of penetration to coating thickness ratio. For a given value of indentation strain the Meyer hardness calculated from the maximum force measured in the impact test is approximately 2.5 times that resulting from the Brinell test. This reflects the fact that the higher strain rate in the impact test would give rise to a higher flow stress and thus hardness.

**Keywords:** Thermoplastic coating; impact tests; indentation tests; impact response; Meyer hardness; Brinell indentation

## **1. Introduction**

Particulate filled or fibre reinforced polymeric composite materials or polymeric coatings have been studied extensively to investigate their structural, thermal, mechanical, tribological, impact, or dielectric properties [1-6] by computational and various experimental methods designed to evaluate the performance of composites or plastic coatings under different test conditions [7-12]. It is generally accepted that the overall behavior of composites or coatings is influenced by the presence of other constituents in the coating (fillers, additives, etc.) [5]. It is not surprising to find that the generic properties of particulate or fibre reinforced polymeric composites or coatings, such as their tensile strength, modulus, impact resistance or fracture toughness, will be enhanced provided that the optimum amount and size of the fillers are incorporated appropriately in the matrix materials [1-2, 13-14]. Most of the previous studies aimed at improving the mechanical properties of composites or polymeric materials or at assessing the newly developed materials have stressed one property and thus used one test method, for example, impact testing, scratch testing or indentation methods [15-19].

Particulate filled fluoropolymer coatings are being widely used in the oil and gas industry for their good corrosion resistance. However, other properties are also often important. For example when these coatings are applied to downhole tubulars wear resistance is also necessary, thus wireline wear tests have been conducted to assess this specific wear problem [4]. In this downhole application damage can also occur by the wireline tools colliding with or indenting the coating. The present research addresses this problem by assessing the resistance of particulate filled fluoropolymer coatings to indentation under both dynamic impact tests and static Brinell indentation tests.

During an indentation test, as the indenter penetrates the coating the material of the coating is displaced radially outwards. When the indenter penetrates through the polymer coating and into the substrate (i.e. when the ratio of the depth of indentation to the coating thickness increases) the coating material displaced by the indenter is squeezed upwards to the surface due to the constraint imposed by the substrate and surrounding coating material. This creates a pile-up of the coating material at the edge of the indenter which affects the load-depth behavior as the contact area is increased by the pile-up and thus the coating can support more load. This explains previous experimental results [18] which suggested that for relatively soft polymers the average indentation pressure is not markedly influenced by

the substrate for depth of indentation/coating thickness values less than 1.0 as the pile-up of coating material, caused by the substrate underneath the indenter, will always support a significant proportion of the load. Even when the depth of indentation/coating thickness is greater than 1 the pile-up of coating will always support a significant proportion of load and thus the hardness measured is not influenced by substrate hardness as much as might be expected if pile-up were not present. Figure 1 shows a schematic diagram explaining the importance of the support provided by the pile-up on the load bearing capacity of the coating during an indentation test under the above two circumstances. If the elastic deformation under indentation is much less than the plastic deformation, then the average indentation pressure (applied load divided by the projected area of contact between the indenter and sample) is equivalent to a measure of the Meyer hardness when the area of contact is measured after unloading. This is the case for glass, but polymers can exhibit viscoelastic recovery after unloading, causing conventional hardness values to increase with time. For example, for epoxy and epoxy acrylate coatings the Vickers hardness was demonstrated to increase by up to about 10% in 30 minutes after unloading, while for a urethane acrylate coating the indent disappeared completely 30 minutes after unloading [18].

The results obtained from standard impact tests are usually a single value such as the energy spent on a particular sample in an impact test. This is of limited value in describing the impact performance of a material. Instrumented impact rigs yield information on forces, velocities, and energies of the impactor [20]. Instrumented impact testing has become an increasingly used technique to obtain complete impact information and to understand fully the impact mechanisms involved [21, 22].

The maximum loading force during an impact test can be correlated with the damage or fracture of the material during an impact test and is thus an important parameter [23]. Vandergheynst et al. [24] described an instrumented falling weight impact test, where a clamped PMMA disk sample is hit by a striker of mass  $M$ . In these instrumented tests a measure of the force, e.g. acceleration, is monitored with time. During the very short time scale of the impact event (of the order of  $10^{-3}$  s), the force  $F$ , the time  $t$  and the initial velocity were recorded. The displacement and energy were calculated from momentum conservation; however, oscillations appeared in the force vs. time curve, giving the impression that high frequency phenomena occurred during this very rapid test [23, 24]. These high frequency signals in the force-time trace make it difficult to determine the maximum loading force from the force-time trace. Therefore, in order to obtain the

maximum loading force during an impact test the high frequency signals have to be removed, by filtering, from the original force-time trace.

As the thickness of the coating and its substrate might influence impact performance as different thicknesses of sample would cause different resonant frequencies and these frequencies may affect the damage observed on the sample tested [25-27], particulate filled thermoplastic fluoropolymer coatings with different thicknesses of the coating layer and steel substrate were tested in this study.

## **2. Experimental**

### **2.1 Characterisation of particulate filled fluoropolymer coatings**

F-4001, a type of particulate filled thermoplastic fluoropolymer coating manufactured by thermal spraying onto a mild steel substrate was used in this study. The coating has a low percentage (2%) of  $\text{CaF}_2$  fillers embedded in the coating matrix with a relatively thick primer layer (~ 0.2 mm) containing 12% SiC fillers. The F-4001 thermoplastic coatings so produced had two thicknesses, 0.5 and 1.5 mm; these were designated F-4001A and F-

4001C respectively. Samples F-4001A are on a 4.5 mm thick steel substrate, and samples F-4001C1 and F-4001C2 are on steel substrates 2 and 4.5 mm thick, respectively. The dimension of each coating sample for the impact test was 38 mm x 38 mm.

## **2.2 Experimental design and instrumentation**

The impact rig used in this study was designed and built at Southampton University. The rig can be classed as a ‘falling-weight’ type of impact rig, as opposed to other standard impact rigs such as those used for Izod or Charpy tests.

Figure 2 presents the arrangement of the impact rig close to the sample to be impacted. The tup is tethered to a 5 mm diameter yachting rope and can be dropped straight through a guide tube from a height of up to 2.75 metres. The tup nose was a 22.2 mm diameter steel ball bearing which acts as the direct impactor on the coating surface. The mass of the tup is 1.9 kg; therefore, different impact energies can be obtained by dropping the tup from different heights. Beneath the guide tube is the sample holder into which the 38 x 38 mm samples are fixed. The flat fluoropolymer coating samples are clamped by the sample holder onto a large block of stainless steel resting on the concrete floor. The sample holder

also contains a 'rebound catcher' used to prevent double impacts on the sample from the rebounding tup during impact tests. The rebound catcher consists of a plate that is driven out to protect the sample by a pneumatic piston activated by a foot pedal.

A Bruel & Kjaer accelerometer type 4369 was used to measure the impact force. The principal advantage of this type of sensor is its ability to sustain high shock acceleration loads (up to 10,000 *g*). The accelerometer produces a voltage signal proportional to acceleration. Knowing the acceleration of the mass in the impact direction the total force on the impactor in the impact direction can be obtained ( $F = ma$ ). The accelerometer used in this study was mounted directly above the tup nose in the housing body of the tup. This is the closest possible location of the accelerometer to the impactor, so it gives the 'cleanest' signal of the impact response without attenuation or distortion. A Kistler 5001 charge amplifier was utilised to integrate the charge developed from the piezoelectric elements in the accelerometer. An output voltage is produced by the charge amplifier which is proportional to the charge received at the input, and therefore to the acceleration of the accelerometer. An A/D converter installed in a Personal Computer (PC) was connected to the output of the Kistler 5001 charge amplifier and used to convert the analogue signals collected from the accelerometer and the charge amplifier to digital codes. The maximum

permissible sampling rate, 250 kHz, of the current recording system was employed in all the impact tests. Preliminary tests had indicated that this sampling rate was high enough to obtain detailed information from the test.

### **2.3 Experimental process**

Samples with various coating and steel substrate thicknesses, i.e. F-4001A, F-4001C1 and F-4001C2, were used in order to assess the main factors influencing the impact resistance of the coatings. The impact energy in the tests is delivered from the gravitational potential energy possessed by the tup, which can be calculated from  $U = mgh$ , where  $m$  is the mass of the tup,  $g$  is the acceleration due to gravity, and  $h$  is the height of the tup. The height to which the tup is elevated for each test can be controlled accurately with a maximum error of  $\pm 5$  mm, which gives an experimental error of less than 1.5% in the potential energy of the tup. Therefore the impact energy applied in each test is repeatable and this experimental error can be neglected. The tup was dropped from different heights in order to obtain an impact energy of 7 to 22 J. Within this energy range quantifiable impact damage, e.g. an impact indent on the coating surface could be obtained for each coating sample. Each impact test was repeated three times and the results recorded and

subsequently analysed. During each impact test, the voltage signal corresponding to the impact response was recorded initially and saved. These voltage signals were then converted into acceleration and force information for further analysis.

### **3. Experimental results and discussion**

#### **3.1 Damage to the coatings on impact testing**

Figures 3 (a) and (b) show the top view and cross section (after sectioning through the indent followed by metallographic preparation) of the typical damage resulting from an impact test on coating F-4001C2 with an impact energy of 14 J. Substantial plastic deformation of the coating surface was observed for the coatings tested and the periphery of the impact indent exhibited pile-up after the impact process. Examination by optical microscopy revealed that no cracks were induced on the coating surfaces and the primer layer was not deformed during the impact tests. No debonding of the polymeric coating from the substrate was noted in any of the impact tests. Examination of the cross-sections also revealed that the fillers contained in both the coating and the primer layers did not seem to affect the damage caused by the impact tests. The diameter and depth of the

impact craters were measured by using a surface profilometer (Form Talysurf – 120). The probe of the profilometer initiated its traverse from one side of the crater produced by the impact test and crossed to the other side along the middle of the crater. The trace of the movement of the probe was recorded automatically on recording paper by the Talysurf, so the diameter and the depth of the crater can be read. The depth of the crater was taken from the lowest point measured on the crater to the level of the edge of the pile-up. Each impact test was repeated three times with the same impact energy, and the average values of the diameter and the depth of the craters were obtained and adopted for further analysis. Table 1 gives the average diameter and the depth of the crater together with their standard deviations for the samples of F-4001 tested under various impact energies. The standard deviations calculated from the individual measurements of the diameter and the depth range from 1.2% to 6.5% of the average value which are relatively small and thus not significant.

### **3.2 Maximum loading force during each impact test**

The Fast Fourier Transform, FFT, method was used to analyse the frequency information in the impact responses. A large number of impact tests on different materials have been carried out on the present impact testing rig and the frequency signals generated by the

impact response compared and studied. High frequency signals of above 4 kHz were found to be dominant in all the impact tests carried out on the different sample materials tested, which indicates that these high frequency signals are related to the test rig rather than the samples tested or the damage induced on the samples. Therefore, the high frequency signals above 4 kHz in each of the present impact responses were filtered from the original force-time traces in order to obtain the maximum loading force generated during the impact test. As each impact test was repeated three times, three readings of the maximum loading force were recorded. Thus Table 1 includes the average maximum loading forces and their standard deviation for impact tests on the fluoropolymer coatings obtained after the high frequency signals had been filtered. The standard deviation for the maximum force ranges from 2.1% to 4.8% of the average value.

### **3.3 Comparison between the impact tests and static indentation tests**

Figure 4 gives the average maximum impact force as a function of the impact energy. The maximum impact force increased with impact energy for all samples tested. It is interesting to note that at the lower impact energy of 10 J the thinner coating with thicker substrate (F-4001A) shows a 17.3% higher maximum force than the thicker coating with thinner

substrate (F-4001C1). This is probably a result of the greater pile up of the coating layer contributing to cushion the impact and greater influence of the stiffer steel substrate for the thinner coating sample. Impact testing the F-4001 thermoplastic coating produced a plastic indentation, i.e. the test is really a form of dynamic hardness testing with a spherical indenter. If the test were conducted statically it would be simply a type of Brinell hardness test. Note the Brinell hardness is load divided by the curved surface of the indentation and is not a pressure. The Meyer hardness is load divided by the cross section area of the indent. The relationship between load,  $P$ , and diameter,  $d$ , of indents produced by spherical indenters can be expressed by Meyer's law [28]. For a ball of fixed diameter,  $P = kd^m$ , where  $k$  is a constant and  $m$  is the Meyer index. Figure 5 shows the average maximum force generated during the impact tests as a function of the diameter of the indents ( $d$ ) produced under each maximum force ( $P$ ). The trendline shown on Figure 5 suggests that the thickness of the coating and the substrate did not seem to affect significantly the diameter of the indent made for a given maximum force. The trendline from all data shown in Figure 5 gives the constant in Meyer's law,  $k$ , as 0.11 and the Meyer index  $m$  as 2.3 under these impact conditions. If data for the 1.5 mm thick coating are analysed separately the corresponding trendline gives the constant  $k$  as 0.16 and the Meyer index,  $m$ , as 2.1. The Meyer index is known to vary from a value of 3 in the elastic stage to a value between 2 for fully work

hardened metals and 2.5 for fully annealed metals at the full plastic stage of indentation at which the total deformation of the material around the indenter is plastic [28]. The present value of 2.3 confirms that indentation is predominantly plastic. However, in the present tests, the impactor is indenting a thermoplastic coating and not a metal as described in [28]. Value of  $m$  between 2.4 and 2.7 were found by Pascoe and Tabor [29] on indentation of a range of polymeric materials. Figure 6 shows the average depth of the indent as a function of the maximum force. The thinner coating, F-4001A, shows a deeper indent for a given maximum force than the thicker coating. This is a reflection of the greater pile-up associated with the thinner coating than for the thicker coating resulting from the polymeric material displaced by the indenter being squeezed upward to the surface due to the constraint imposed by the substrate and the surrounding coating material. This is in agreement with the results shown in Figure 4 that indicated that the thinner coating may affect more the maximum force measured. Figure 7 shows the average indentation pressure (i.e. Meyer hardness) calculated from the maximum force and the residual indent size as a function of the depth/coating thickness ratio. All of the values of the depth/coating thickness ratio are greater than 0.125 the value below which the Brinell Hardness Test Method [30] indicates that the hardness measured for metallic materials can be taken to be independent of the thickness of the sample. The depth of indent to coating thickness ratios

for F-4001A, the 0.5 mm thick coating, are particularly high as the small thickness of the coating generated a large piled-up edge to which the depth measurements were related. However, the average indentation pressure (Meyer hardness) does not change markedly as the depth of indent/coating thickness ratio increases. This is in agreement with the result obtained by Ritter [18] discussed in the Introduction.

Standard Brinell hardness tests were carried out on the 0.5 mm and 1.5 mm thick F-4001 thermoplastic coatings under different loads in order to complement the results of the impact test. A 2 mm diameter ball was used for the Brinell tests. Due to the small percentage of fillers in the coating layer and their relatively small size, there was no difference of the hardness values observed when the indents were made at different positions under the same conditions. The diameter of the indents made on the coating surface was measured immediately after indentation and 68 hours later. Figure 8 shows the diameter of indents as a function of the load applied for the 0.5 mm and 1.5 mm thick F-4001 thermoplastic coatings measured immediately after the Brinell hardness test and the corresponding Meyer's law equations. For a given indentation load, the diameter of indents made on the 1.5 mm thick coating are noted to be slightly larger than those made on the 0.5 mm thick coating reflecting the greater influence of the substrate on the hardness measured

for the thinner coating thickness. Figure 9 presents the diameter of indents measured both immediately after indentation and 68 hours later for the 0.5 mm thick coating as a function of load applied. For all indents except those made with a maximum load of approximately 0.5 kN there is no significant difference in the measurements made immediately after the indentation and 68 hours later implying that there was no obvious relaxation of the indents after the load has been removed. Similar results were obtained for the 1.5 mm thick coating. This agrees with previous work for polymer materials which found that for a Vickers indent [31] there no recovery along the indent diagonals and for a spherical indent there was little change in depth [32]. The constant  $k$  in the Meyer's law equation for the Brinell hardness tests on all the coatings ranged from 0.065 to 0.078 whereas the Meyer index  $m$  was between 2.25 and 2.91. Taking all the Brinell hardness data together,  $k = 0.072$  and  $m = 2.7$ . This should be compared with  $k = 0.11$  and  $m = 2.3$  under impact conditions. Considering first the effect of the diameter of the indenter/impactor, Meyer found that  $m$  was almost independent of the diameter,  $D$ , of the indenter but the constant  $k$  decreased with increasing diameter,  $D$ , such that

$$X_m = k_1 D_1^{m-2} = k_2 D_2^{m-2} = k_3 D_3^{m-2}$$

where  $X_m$  is a constant. The value of  $m$  found for the two different diameters of impactors is similar. However, the value of  $k$  from the impact results with the larger diameter impactor would be expected to be smaller than that for the Brinell results. The reverse is found. If  $m$  is taken as 2.5 (the average value from the impact and Brinell hardness results), the ratio of the constants from the Brinell and impact tests would be expected to be 3.3 whereas the ratio found is 0.65. This will be discussed later. Figure 10 presents the effect of the depth of indent/thickness of coating on the Meyer Hardness calculated from the Brinell indents. The Meyer hardness is noted to increase as the depth/coating thickness ratio increases. This was not observed for the corresponding data from the impact indents, Figure 7.

Tabor proposed for metals that the strain at the edge of a spherical indentation is proportional to the ratio of the contact area diameter to the indenter diameter [33]. This was called the representative strain,  $\varepsilon_r$ , and is calculated from  $\varepsilon_r = 0.2 \frac{a_c}{R}$ , where  $a_c$  is the radius of the indent and  $R$  is the radius of the indenter. This relationship has recently been shown to be also applicable to polymeric materials [34, 35]. In general, the value of the strain at the indentation perimeter depends on the angle between the indenter surface, at the contact edge, and the original surface plane. Therefore, the strain produced by sharp

indenters is of a constant value which is related to the included angle of the indenter tip and is independent of the indentation depth. However, in the case of indentation using a spherical indenter, the angle between the indenter surface, at the contact edge, and the original surface increases with indentation depth, as would the corresponding representative strain. Hence, the strain produced by spherical indenters depends on depth of penetration. Figure 11 shows the Meyer hardness values produced by both the impact and Brinell tests (data for measurements taken after 68 hours given) as a function of the representative strain of each indents for all the F-4001 thermoplastic coatings. For a given value of representative strain the Meyer hardness values from the impact test are seen to be a factor of approximately 2.5 higher than those from the Brinell tests. However, the impact tests result in the sudden application of a load whereas in the Brinell test the load is applied much more slowly. The strain rate in the impact tests was calculated as approximately  $600 \text{ s}^{-1}$  whereas the strain rate in the Brinell hardness test is estimated to be approximately four orders of magnitude smaller. The flow stress of a polymer is known to vary with strain rate, for example Brown et al. [36] found that the maximum flow stress of the fluoropolymers PTFE 7C and Kel-F 81 at  $20 \text{ }^\circ\text{C}$  increase by a factor of approximately 2.7 and 3.4 respectively for a six order increase of strain rate. Thus the factor of 2.5 difference in Meyer hardness observed in the present work could well arise from the difference in

strain rate between the two tests. In general, the values of the Meyer hardness from the Brinell hardness test increase with the increasing representative indentation strain while the results from the impact tests show little change, albeit over a smaller indentation strain range. The stress field from the larger diameter ball (22.2 mm) used in the impact test will extend to a greater distance than that from the small ball (2 mm) used in the Brinell hardness test. Hence at a given representative strain value the stress field from the larger ball will extend to a greater depth and so will take into account more the substrate. At low loads the stress field from the small 2 mm diameter ball used in the Brinell hardness test will be largely confined to the coating and hence a smaller value of Meyer hardness will be obtained. As the load in the Brinell test is increased and the strain of the indent increases and the stress field from the ball will extend into the substrate and the hardness will thus increase.

#### **4. Conclusions**

Particulate filled thermoplastic fluoropolymer coatings with different coating thicknesses and different substrate thicknesses have been tested under the impact testing conditions.

Brinell indentation tests have been carried out in order to compare the hardness values of

the coatings samples under different strain rates. The following main conclusions can be drawn from the analysis of the test results:

1. The experimental process designed to impact test the polymeric coatings gives results where the experimental and measurement errors were not significant compared with the calculated average values.
2. The fillers in the coating material do not affect the damage seen on the coatings after the impact tests.
3. The coating thickness and the substrate thickness have little effect on the diameter of the indents produced by the same impact force during the impact tests; however, the thinner coating shows a deeper indent than the thicker coating for a given maximum force. This is a reflection of the greater pile-up associated with the thinner coating than for the thicker coating resulting from the polymeric material displaced by the indenter being squeezed upward to the surface due to the constraint imposed by the substrate and the surrounding coating material.
4. The Meyer hardness calculated from the impact tests does not change markedly as a function of the ratio of depth of penetration to thickness of coating. The Meyer hardness calculated from the Brinell test increases with increasing penetration depth.

This reflects an increasing contribution from the substrate as the indentation depth increases.

5. For a given value of indentation strain the Meyer hardness calculated from the maximum force measured in the impact test is approximately 2.5 times that resulting from the Brinell test. This reflects the fact that the higher strain rate in the impact test would give rise to a higher flow stress and thus hardness.

### **Acknowledgements**

Authors acknowledge financial support from the School of Engineering Sciences, University of Southampton and B. P Exploration, Sunbury-on-Thames, UK.

## REFERENCES:

- [1] Ghalia MA, Hassan A, Yussuf A. Mechanical and thermal properties of calcium carbonate-filled PP/LLDPE composite. *J Appl Polym Sci* 2011; 121: 2413–2421.
- [2] Lopresto V, Leone C, De Iorio I. Mechanical characterisation of basalt fibre reinforced plastic. *Composites: Part B* 2011; 42: 717–723.
- [3] Li J. The impact and tribological properties of PTFE composites filled with PA6. *J Termoplast Compos Mater* 2010; 23: 807–816.
- [4] Xu Y, Mellor BG. A comparative study of the wear resistance of thermoplastic and thermoset coatings. *Wear* 2003; 255: 722–733.
- [5] Kouloumbi N, Ghivalos LG, Pantazopoulou P. Determination of the performance of epoxy coatings containing feldspars filler. *Pigm Resin Technol* 2005; 34/3: 148–153.
- [6] Li J. The impact properties of a polyurethane composite filled with clay. *New and Adv Mater* 2011; 197-198: 1100–1103.
- [7] Altaf K, Ashcroft IA, Hague R. Modelling the effect of moisture on the depth sensing indentation response of a stereolithography polymer. *Comp Mater Sci* 2012; 52: 112–117.

- [8] Chan EP, Hu Y, Johnson PM, et al. Spherical indentation testing of poroelastic relaxations in thin hydrogel layers. *Soft Mater* 2012; 5: 1492-1498.
- [9] Xu Y, Mellor BG. Application of acoustic emission to detect damage mechanisms of particulate filled thermoset polymeric coatings in four point bend tests. *Surf Coat Tech* 2011; 205: 5478–5482.
- [10] Nayak R, Dora P T, Satapathy A. A computational and experimental investigation on thermal conductivity of particle reinforced epoxy composites. *Comp Mater Sci* 2010; 48: 576–581.
- [11] Khan SU, Iqbal K, Munir A, et al. Quasi-static and impact fracture behaviors of CFRPs with nanoclay-filled epoxy matrix. *Composites: Part A* 2011; 42: 253–264.
- [12] Suzuki Y, Todoroki A, Matsuzaki R, et al. Impact-damage visualization in CFRP by resistive heating: Development of a new detection method for indentations caused by impact loads. *Composites: Part A* 2012; 43: 53–64.
- [13] Ashori A. Effects of particle size and coupling agent concentration on mechanical properties of particulate-filled polymer composites. *J Thermoplast Compos Mater* 2010; 23: 169–174.

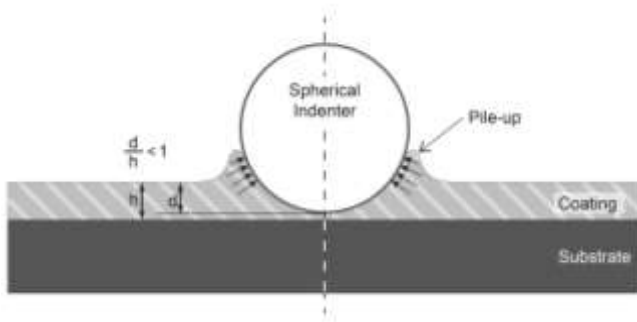
- [14] Melo J, Santos E. Mechanical and microstructural evaluation of polymer matrix composites filled with recycled industrial waste. *J Reinf Plast Comp* 2009; 28: 2459–2471.
- [15] Peng X, Huang J, Deng H, et al. A multi-sphere indentation method to determine Young's modulus of soft polymeric materials based on the Johnson–Kendall–Roberts contact model. *Meas Sci Technol* 2011; 22: 1–6.
- [16] Perfetti G, Arfsten J, Kwade A, Wildeboer WJ, et al. Repeated impacts tests and nanoindentation as complementary tools for mechanical characterization of polymer-coated particles. *J Appl Polym Sci* 2010; 118: 790–804.
- [17] Cheng L, Gerberich WW. Spherical-tip indentation of viscoelastic material. *Mech Mater* 2005; 37: 213–226.
- [18] Ritter JE, Siou DR, Lardner TJ. Indentation behavior of polymer coatings on glass. *Polym Eng Sci* 1992; 32: 1366–1371.
- [19] Warren R. Measurement of the fracture properties of brittle solids by Hertzian indentation. *Acta Metall Mater* 1978; 26: 1759–1769.
- [20] Zoller P. Instrumentation for impact testing of plastics. *Polym Test* 1983; 3: 197–208.

- [21] Keledi G, Sudár A, Renner K, et al. Tensile and impact properties of three-component PP/wood/elastomer composites. *Express Polym Lett* 2012; 6: 224–236.
- [22] Raghavan J, Bartkiewicz T, Boyko S, et al. Damping, tensile, and impact properties of superelastic shape memory alloy (SMA) fiber-reinforced polymer composites. *Composites: Part B* 2010; 41: 214–222.
- [23] Kalthoff JF. On the validity of impact energies measured with polymeric specimens in instrumented impact tests. *Impact and Dynamic Fracture of Polymers and Composites* 1995; ESIS 19: 21–31.
- [24] Vandergheynst P, Goldberg A, Doghri I, et al. Modeling and simulation of an impact test using wavelets, analytical solutions and finite elements. *Int J Solids Struct* 2001; 38: 5481–5508.
- [25] Kim MS, Shin HS, Lee HC. The effect of back plate materials on perfect cone formation in impact-loaded soda-lime glass. *Int J Impact Eng* 2003; 28: 281–290.
- [26] Zhao YB, Wei GW, Xiang Y. Discrete singular convolution for the prediction of high frequency vibration of plates. *Int J Solids Struct* 2002; 39: 65–88.
- [27] Kobayashi S, Kawahara M. Effects of stacking thickness on the damage behavior in CFRP composite cylinders subjected to out-of-plane loading. *Composites: Part A* 2012; 43: 231–237.

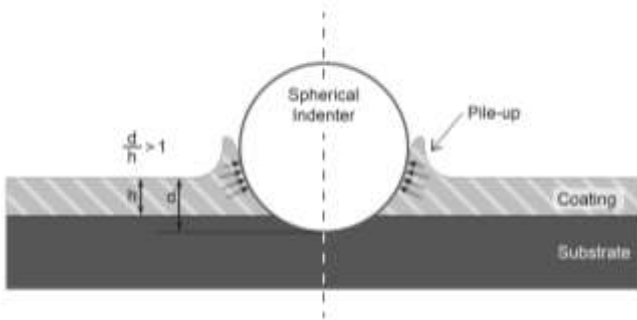
- [28] Meyer E, Zeits D. Vereines Deutsch Ingenieure 1908; 52: 645.
- [29] Pascoe MW, Tabor D. The friction and deformation of polymers. Proc R Soc London, A 24 1956; 235: 210–224.
- [30] BS EN ISO 6506-1:1999 Metallic Materials Brinell hardness test method.
- [31] Low IM, Shi C. Vickers indentation responses of epoxy polymers. J Mater Sci Lett 1998; 17: 1181–1183.
- [32] Kolarik J, Pegoretti A. Indentation creep of heterogeneous blends of poly(ethylene terephthalate)/impact modifier. Polym Testing 2004; 23: 113–121.
- [33] Tabor D. The Hardness of Metals. Clarendon Press, Oxford, 1951:94.
- [34] Pelletier H, Gauthier C, Schirrer R. Experimental measurement and numerical simulation of the plastic strain during indentation and scratch tests on polymeric surfaces. J Mater Res 2009; 24: 1169–1181.
- [35] Chatel T, Pelletier H, Houérou V, et al. Original in situ observations of creep during indentation and recovery of the residual imprint on amorphous polymer. J Mater Res 2012; 27: 12–19.
- [36] Brown EN, Rae PJ, Gray GT. The influence of temperature and strain rate on the tensile and compressive constitutive response of four fluoropolymers. Journal de Physique IV 2006; 134: 935–940.

**Table 1. Diameter, depth of the crater and maximum impact force measured for tests carried out on coating F-4001 at various impact energies.**

Impact energy, J	F-4001A			F-4001C1			F-4001C2		
	Diameter, mm	Depth, mm	Maximum loading force, kN	Diameter, mm	Depth, mm	Maximum loading force, kN	Diameter, mm	Depth, mm	Maximum loading force, kN
7	$6.70 \pm 0.2$	$0.55 \pm 0.036$	$7.5 \pm 0.36$	—	—	—	—	—	—
10	$7.0 \pm 0.26$	$0.62 \pm 0.03$	$9.5 \pm 0.26$	$6.60 \pm 0.1$	$0.44 \pm 0.052$	$8.1 \pm 0.35$	—	—	—
14	—	—	—	$7.80 \pm 0.46$	$0.60 \pm 0.01$	$11.5 \pm 0.7$	$7.30 \pm 0.44$	$0.54 \pm 0.02$	$10.5 \pm 0.46$
22	—	—	—	$8.50 \pm 0.36$	$0.80 \pm 0.026$	$13.6 \pm 0.46$	$8.20 \pm 0.35$	$0.74 \pm 0.046$	$13.4 \pm 0.29$



(a) depth of indentation/thickness of coating  $< 1.0$ .



(b) depth of indentation/thickness of coating  $> 1.0$ .

Figure 1 Schematic diagram showing the support from the pile-up to the load exerted by the spherical indenter during an indentation test.

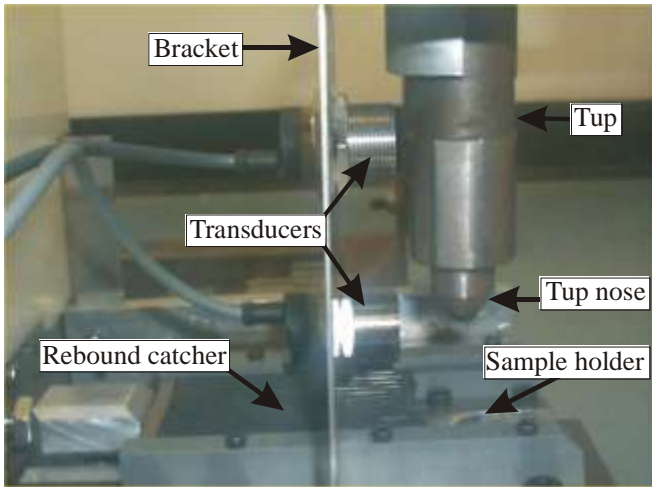
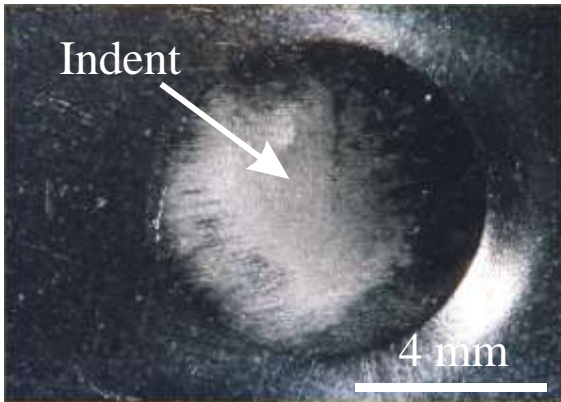
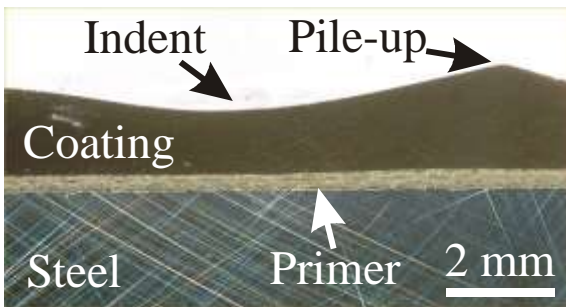


Figure 2 Arrangement of the impact test rig for the particulate filled thermoplastic fluopolymer coatings.



(a) Top view of the indent on the coating surface.



(b) Cross section of the indent on the coating surface.

Figure 3 Typical damage from an impact test on coating F-4001C2 with an impact energy of 14 J. Note the plastic deformation of the coating surface and the pile-up around the indent.

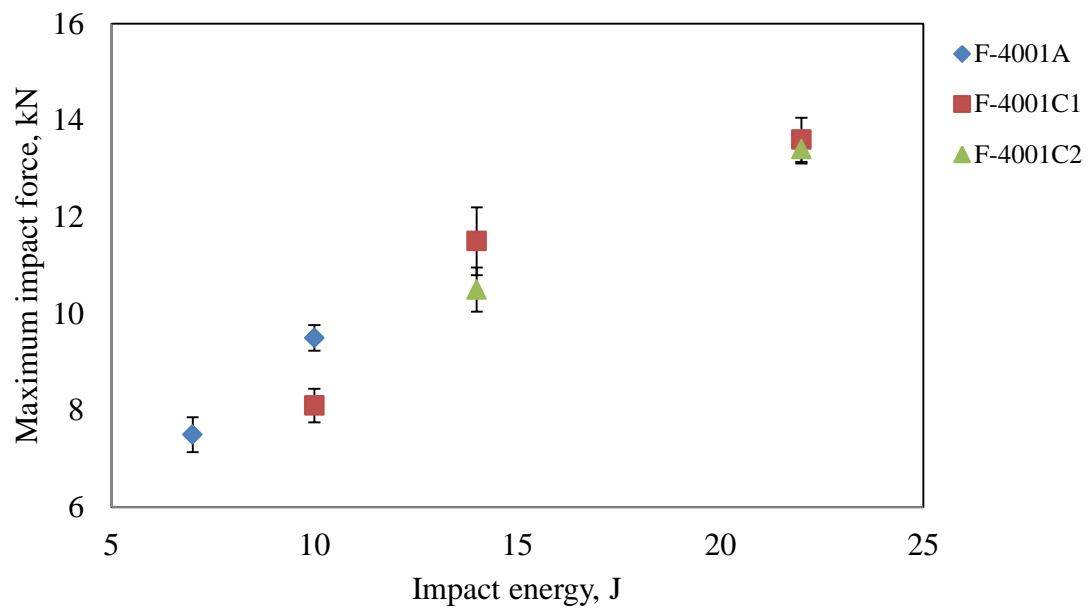


Figure 4 The maximum impact force determined in the impact tests as a function of impact energy.

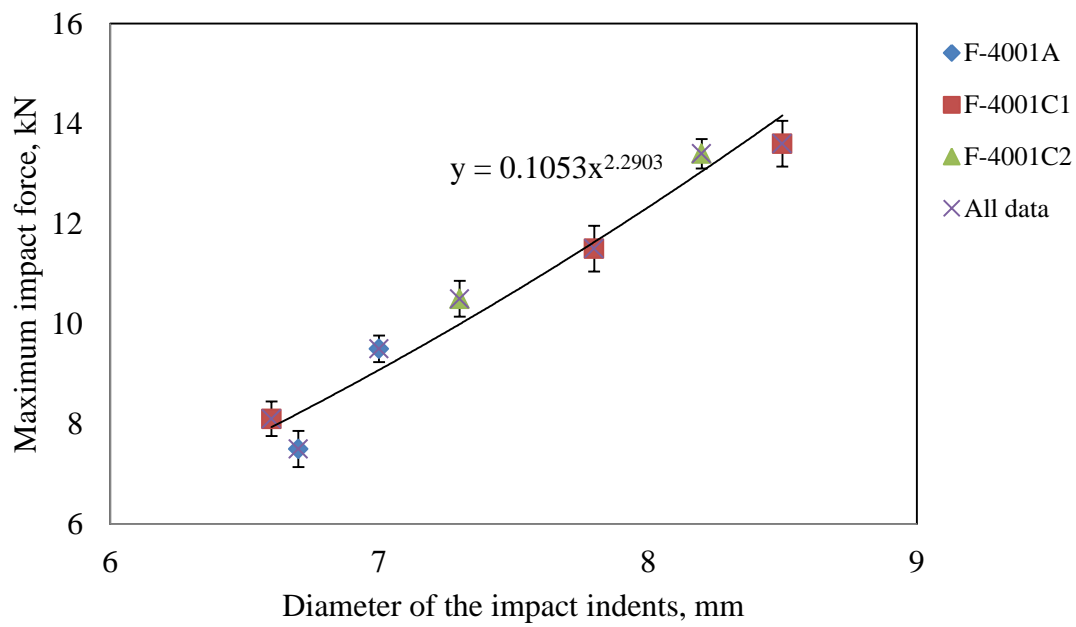


Figure 5 The diameter of the impact indents as a function of the maximum impact force measured.

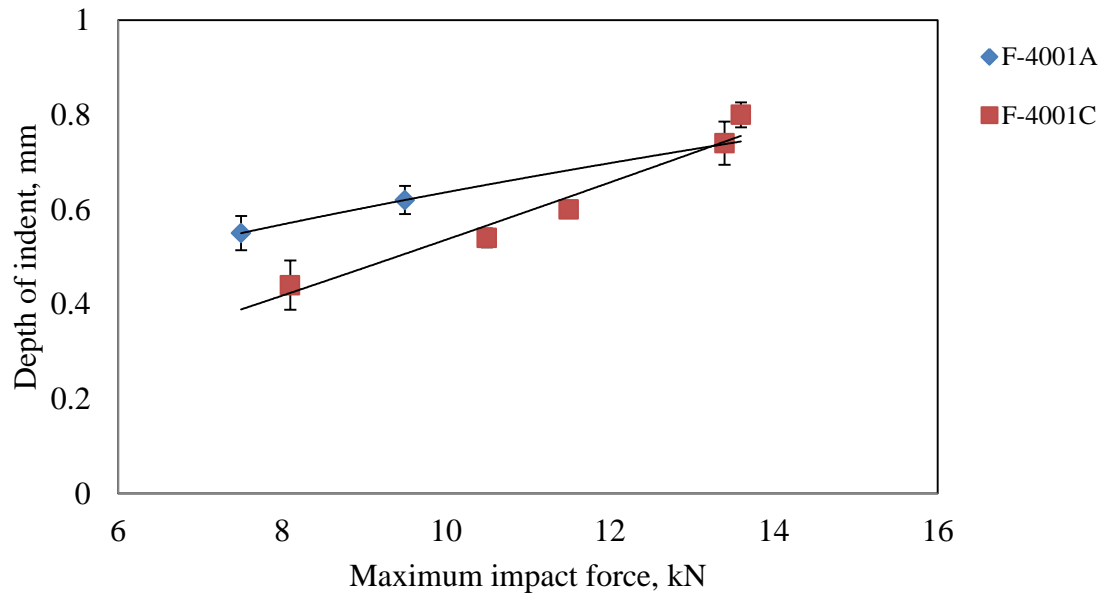


Figure 6 Depth of the impact indents as a function of the maximum impact force.

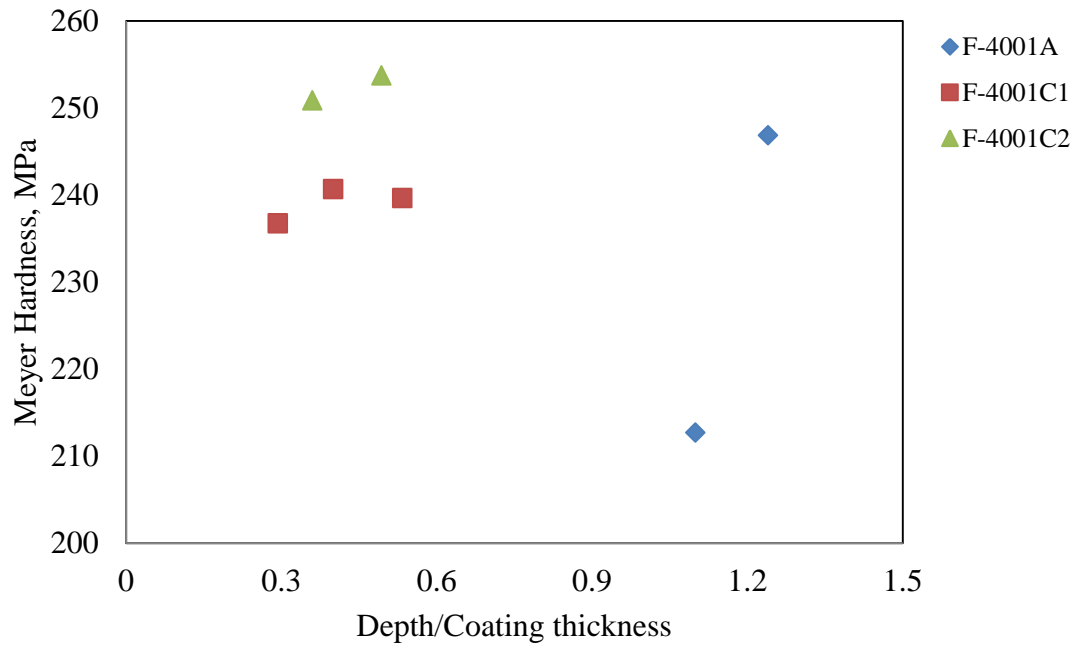


Figure 7 Meyer hardness from the impact tests as a function of the depth /coating thickness ratio.

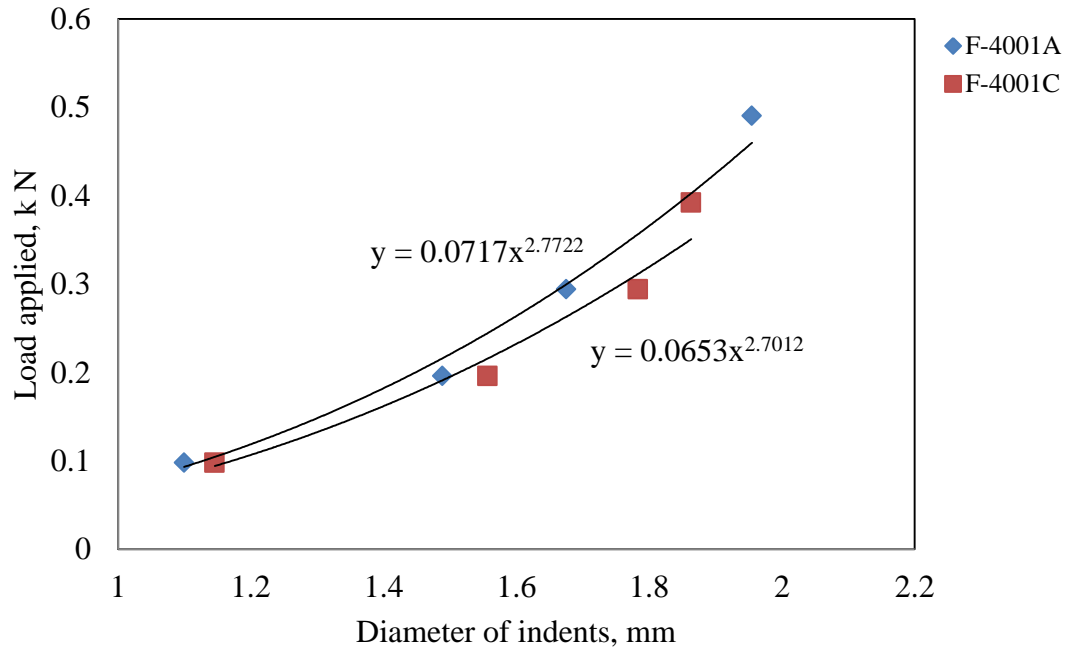


Figure 8 Diameter of Brinell indents measured immediately after indentation as a function of the load applied for 0.5 and 1.5 mm thick coatings.

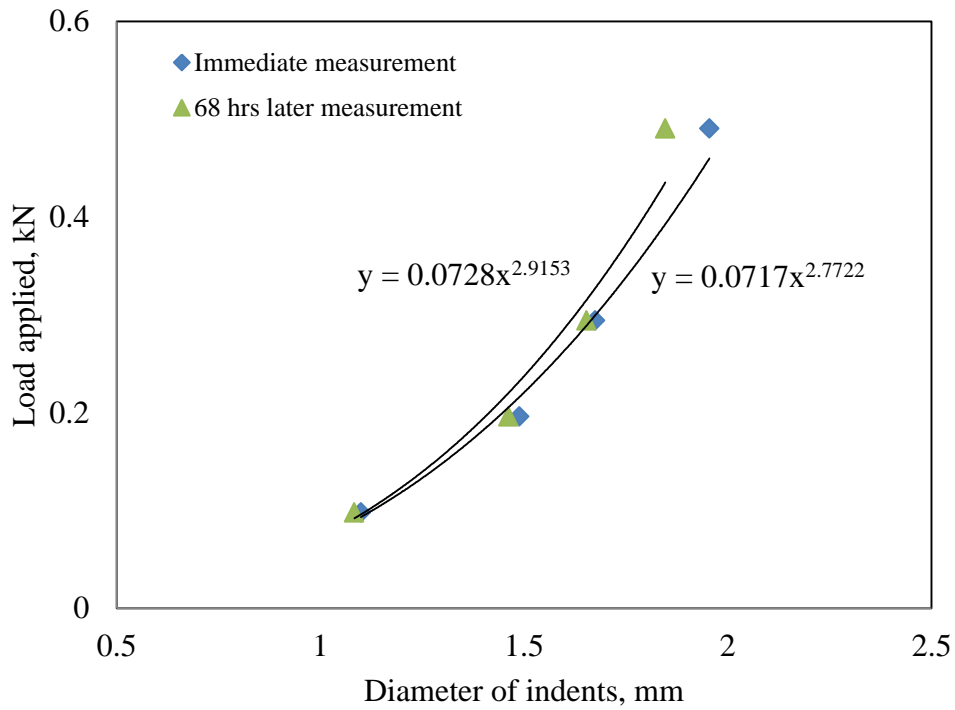


Figure 9 Diameter of Brinell indents measured immediately after indentation and 68 hours later as a function of the load applied for the 0.5 mm thick F-4001A coating.

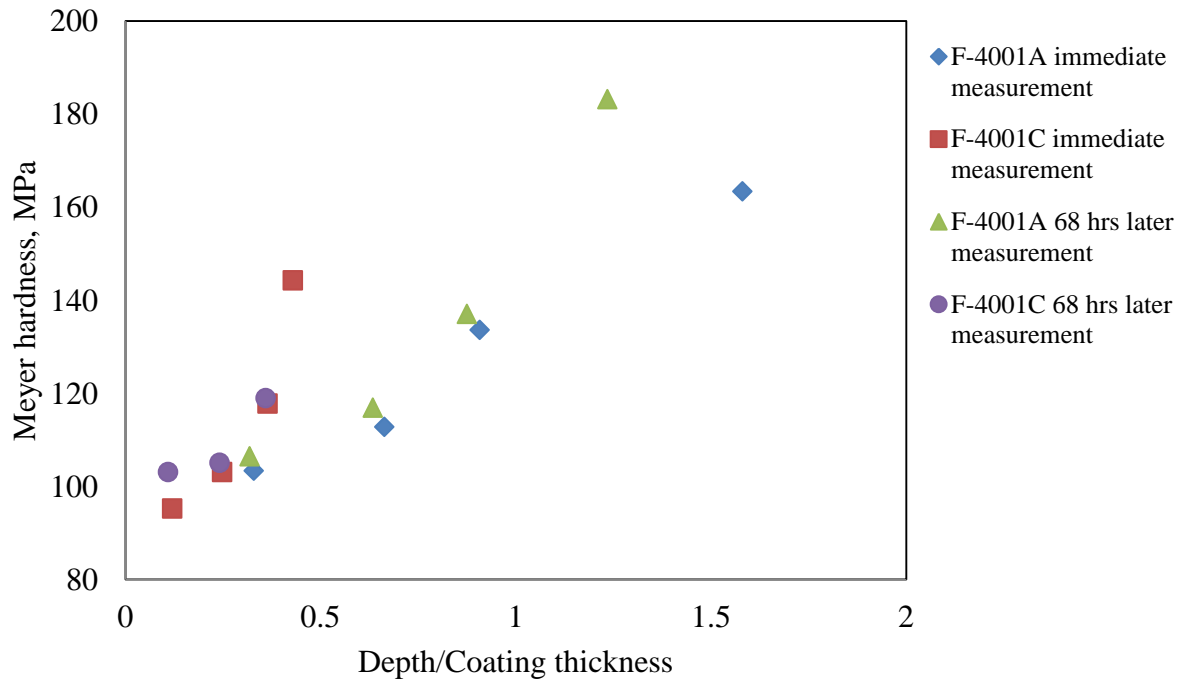


Figure 10 Meyer hardness as a function of the indent depth/coating thickness ratio for the Brinell hardness indents.

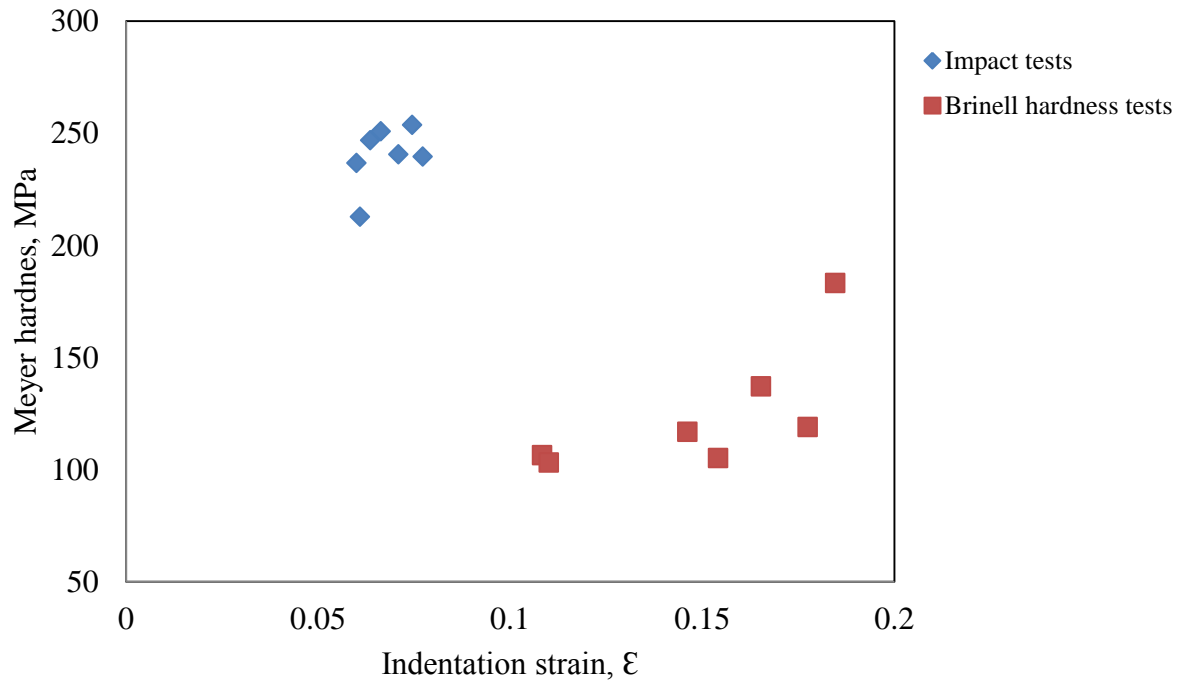


Figure 11 Meyer hardness as a function of indentation strain for both the impact and Brinell hardness (measured immediately after indentation) test results.